Structure and magnetic properties of multi-walled carbon nanotubes modified with cobalt

U. Ritter [a,*], P. Scharff [a], G.E. Grechnev [b], V.A. Desnenko [b], A.V. Fedorchenko [b], A.S. Panfilov [b], Yu.I. Prylutskyy [c], Yu.A. Kolesnichenko [b]

[a] Ilmenau Technical University, Department of Chemistry, Weimarer Str. 25, 98683 Ilmenau, Germany
[b] B. Verkin Institute for Low Temperature Physics and Engineering of the NASU, Lenin Ave. 47, 61103 Kharkiv, Ukraine
[c] Kyiv National Taras Shevchenko University, Department of Biophysics, Volodymyrska Str. 64, 01601 Kyiv, Ukraine

ARTICLE INFO

ABSTRACT

The magnetic properties of multi-walled carbon nanotubes (MWCNTs) modified with cobalt nanoparticles were studied in the temperatures and magnetic field range of (4.2–290) K and (0.03–5) T, respectively. Nanoparticles of cobalt encapsulated inside MWCNTs were obtained by using the chemical vapor deposition technique. The low temperature SQUID magnetization measurements were supplemented with structural investigations by means of high-resolution transmission electron microscopy, scanning electron microscopy as well as thermogravimetric and X-ray diffraction analysis. X-ray diffraction revealed the presence of MWCNTs, f.c.c. Co and h.c.p. Co phases. The magnetic characterization provided the remanent magnetization value (M_R) of about 0.07 emu/g ($\sim$40% of the saturation moment), while the coercive field (H_C) value amounts to 600 Oe. Both parameters M_R and H_C slightly decrease with the rise of temperature. The substantial magnetization increase observed at low temperatures suggests the existence of nano Co clusters (in the atomic scale size).

1. Introduction

Carbon nanotubes (CNTs) exhibit unique combination of physical properties [1–3], in particular, they are chemically and thermally stable and are characterized by high mechanical strength, thermal and electrical conductivity, and large specific surface area. At the present CNTs are considered as the most promising building blocks for nanoelectronic devices, since they are able to form a perfect spin-transport medium with a long spin relaxation time and weak spin–orbital coupling. It has been shown that in specific types of CNTs the mean free path of a conduction electron increases with the diameter of the tube leading to quasi one-dimensional and ballistic transport of electrons [3]. The aspect of ballistic transport supports the important property of CNTs – low and constant resistivity. Also, even pure CNTs, which are non-magnetic materials, are characterized by a giant magneto-resistance [4,5].

On the other hand, it is quite apparent that modification of CNTs by intercalation and filling the internal cavities with different elements would lead to significant differences in their electronic structure, transport and magnetic properties [6–11]. Due to very large magnetic shape anisotropies, the encapsulation of magnetic phases in CNTs could provide a feasible

approach to achieve a stabilization of magnetic order against the thermal fluctuations in systems having extremely reduced dimensions. Also, the ferromagnetic (FM) nanoclusters are expected to have much better magnetic properties than bulk metals due to their single domain nature [12]. Therefore, it is desirable to produce CNTs with magnetic material inside of the tubes in a specific and controlled way.

Beyond the geometrical advantage of a quasi one-dimensional CNT design, the carbon shells can provide an effective protection against oxidation. This is particularly important, since applications of ferromagnetic nanoclusters are limited due to air oxidation, and for practical usage it is needed to coat metal nanoparticles with air-stable materials. Therefore carbon-encapsulated magnetic nanoparticles have received considerable attention due to their high chemical and thermal stabilities [13,14]. The promising applications of magnetic encapsulates include magnetic data recording, magnetic resonance imaging, and also magnetic carriers in the field of biomedicine (e.g. transport of anticancer drugs and heat treatment of tumors [14]). Also, the magnetic nanoclusters packed inside of carbon nanotubes can provide a substantial spin polarization at the Fermi level. Therefore such metal-filled carbon nanotubes can be considered as potential devices for spin-polarized transport and applications in the field of spintronics.

Finally, except for the interest related to practical applications, a study of these magnetic systems provides an avenue for the exploration of the magnetic order physics in close-to-one-dimensional structures. In particular, one can expect a substantial effect of magnetic fluctuations due to the reduced dimension of nanostructures.

Thus, the purpose of the present work is the investigation of the structural characteristics and magnetic properties of multi-walled carbon nanotubes (MWCNTs) modified with cobalt nanoparticles in a range of temperatures (4.2–290) K and magnetic fields (0.03–5) T. Apparently, the magnetic properties of this system have to be studied and discussed in relation to the respective structural characteristics.

2. Experimental details

Chemical vapor deposition (CVD) was employed to produce CNTs filled with cobalt nano-particles. Essentially, the growth process involved heating of a catalyst material to high temperatures in a tube furnace. It was followed by the injection of a hydrocarbon gas, being the carbon source, through the tube reactor for a chosen growth time. Then, under the flow of an inert gas, to prevent oxidation of the carbon species, the system was cooled down to the room temperature and the carbonaceous materials grown over the catalyst were collected.

In the course of CNT growth the key parameters were the chosen hydrocarbons, catalysts and the growth temperature, which independently determined properties of the obtained tubes. Our method was based on the catalytic decomposition of benzene (as carbon source) and cobalt acetylacetonate (as cobalt source) of in a tube furnace at different temperatures. CNTs have been synthesized by simultaneous deposition of catalytic amounts of cobalt and carbon on the walls of a quartz tube reactor. With this process, the cobalt acetylacetonate is decomposed and provides the cobalt particles which are required for the nucleation of the CNT. After the reaction cobalt clusters were found inside the CNTs, whereas the aligned nanotubes have grown on the quartz glass reactor wall. The tube reactor has been placed in a furnace at 900 °C and connected to a gas inlet system. The synthetic route involved the spray pyrolysis of a cobalt acetylacetonate/benzene solution in an Ar atmosphere. In order to obtain short and well defined CNT the spraying time was kept between 1 and 4 min. The control of the CNT length and diameter was performed through the spraying time, the argon flow and the concentration of the catalyst solution. After slowly cooling down the furnace under argon flow (20 °C/min) the CNTs formed well defined aligned layers on the tube walls, which were then mechanically removed from the tube.

The characterization of the product was performed by a scanning electron microscope (SEM, FEI XL30 LaB$_6$). The samples have been glued to an alumina holder with silver paste and covered by 10 nm thick gold/palladium layers in an ion beam evaporator for contrast and stability reasons. Measurements have been done with different acceleration voltages and variable electron spot size between 5 and 20 nm, depending on the magnification. High-resolution transmission electron microscopy (HRTEM) was carried out with a Philips TECNAI 20 S-TWIN apparatus with field emission gun at 200 kV. The obtained micrographs have been recorded with a 1024×1024 pixel CCD-Camera. For the CNT characterization, the attained resolution (line resolution 0.14 nm, point resolution 0.24 nm) was suitable to resolve single carbon layers, and magnifications of up to 690,000×s have been achieved.

For characterization of the samples, we also employed the thermogravimetric analysis (TG, Sartorius MC5) in air. Their structure and phase composition were studied in detail by the X-ray diffraction spectroscopy (XRD) with X-ray diffractometer (Bruker AXS).

In the temperature range (4.2–290) K the magnetic properties of the cobalt filled MWCNTs were measured by a SQUID (Superconducting Quantum Interference Device) magnetometer [15] in fields up to 50 kOe with an absolute error less than 10^{-6} emu for the measured magnetic moments. For the magnetization studies the samples were prepared by compacting the Co-encapsulated MWCNT powder (mass about 10 mg) inside of an elongated aluminum foil cylinder with 1.5 and 7 mm in diameter and height, respectively. Cylindrical shape of the samples fits the experimental setup and also reduces the effect of demagnetization factor in magnetization data obtained in the magnetic field applied for all measurements along the cylinder axis. The measurements were made after cooling the sample from room to helium temperature in a zero magnetic field (zero-field-cooling regime, ZFC). Then the temperature dependences of the magnetization M(T) were measured under a slow heating with the rate of about 1.5 K/min in the applied magnetic fields H = 300 Oe and 30 kOe. The field dependencies of the magnetization were also measured in ZFC regime in magnetic fields up to 46 kOe at temperatures T = 5, 130 and 250 K.

3. Results and discussion

3.1. Structural properties

According to the electron microscopic SEM and HRTEM results in Fig. 1, the obtained CNT are MWCNTs. The inner diameter of these MWCNTs was estimated to be about (10–12) nm, whereas the outer diameter is about (30–40) nm and the length is up to 30 μm. These MWCNTs contain clusters of cobalt (or its compounds) with an average diameter of (3–5) nm. The SEM and HRTEM images given in Fig. 1 exhibit the absence of amorphous carbon and graphitic particles in the samples.

Results of the thermogravimetric (TG) analysis in Fig. 2 show that the decomposition of the MWCNTs in air starts at temperature about 420 °C, and the overall amount of residue (mostly cobalt oxides) in the MWCNT sample is about 2 wt.%. Also, the TG diagrams demonstrate that the quality of the obtained MWCNTs is high, and the amount of amorphous carbon is very low. It is important to note that accord-
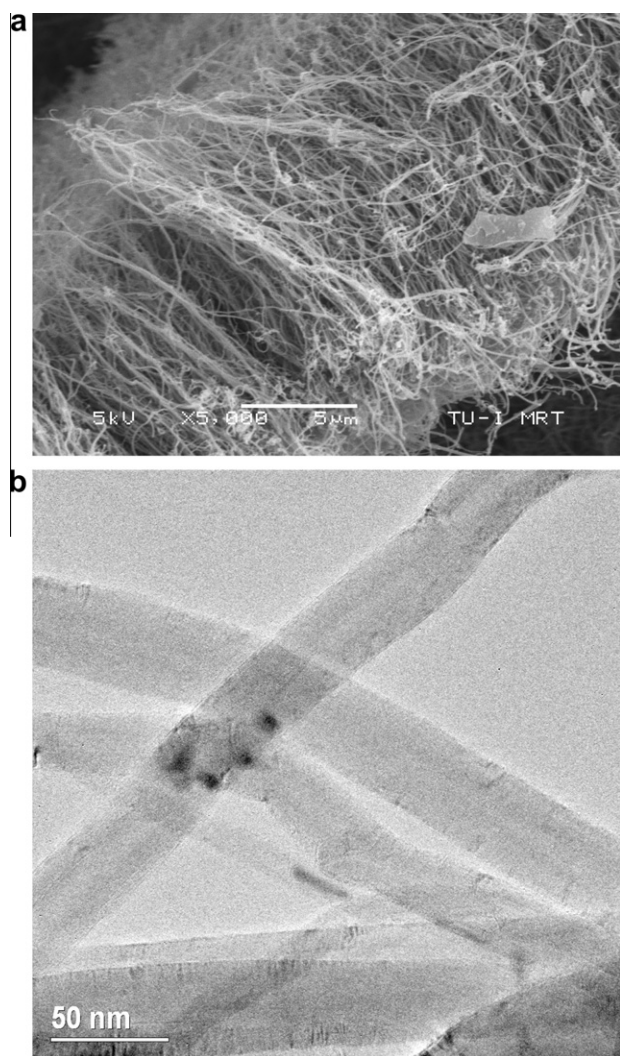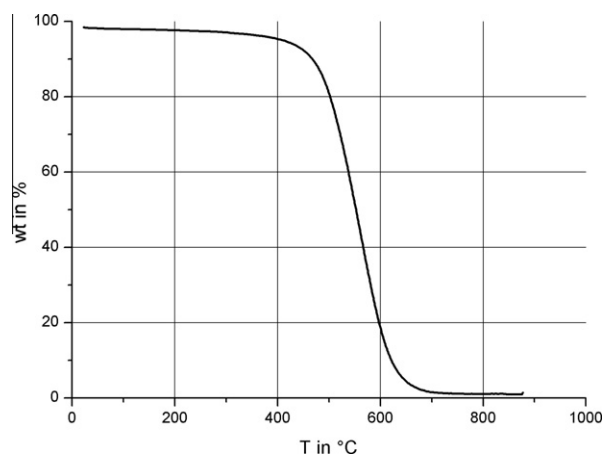

Fig. 2 – Thermogravimetric analysis of MWCNT/Co.

ing to the SEM and TG results, the content of MWCNTs in the samples was estimated to be higher than 90%. The diameter of the formed MWCNTs was found to be directly related to the cobalt cluster diameter, thus an increase of the MWCNT diameter with increasing the cobalt acetylacetonate concentration was observed.

The XRD patterns of MWCNTs grown with benzene (BZ) and cobalt catalyst are displayed in Fig. 3. The peak at the angle of 26.2° corresponds to the interplanar spacing between the MWCNT walls and is marked by CNT (0 0 2). The interlayer spacing of 3.411 Å for MWCNT grown with BZ, slightly exceeds that observed for the perfect graphite (3.354 Å). The other feature characteristic of MWCNTs is the peak at $2\theta = 42.5°$ which corresponds to the (1 0 0) reflection. A peak at the angle of $2\theta = 44.5°$ corresponds to the hexagonal Co reflection. The cubic cobalt reflection at 44.0° is superimposed by a stronger MWCNT (1 0 0) feature. The crystalline phase of hexagonal cobalt is also represented by a weak reflection which is represented by additional peak at 47.5°. Another distinct feature observed in the recorded patterns is the peak from residue cubic iron, at 65.0°. We should note that any characteristic reflections of related oxides or carbides were not observed in the XRD patterns.
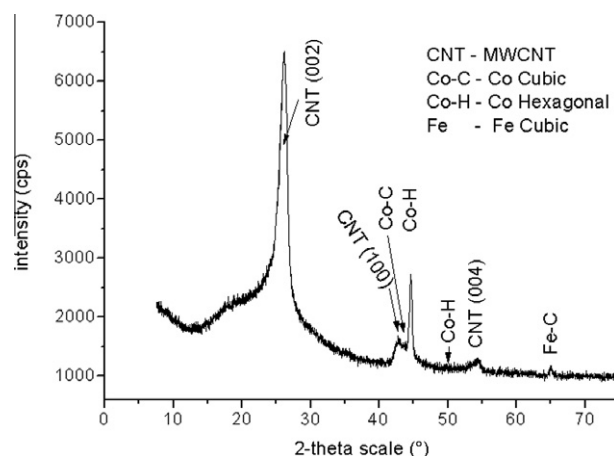

Fig. 1 – SEM and HRTEM images of MWCNT/Co. The dark spots denote the metal nanoparticles.

Fig. 3 – XRD pattern for MWCNT/Co.

3.2. Magnetic properties

In order to characterize magnetic properties of the MWCNT/Co sample, both magnetization curves and hysteresis loops were measured. The results of our magnetization measurements at different temperatures (ZFC regime) are presented in Fig. 4. As it can be seen, the saturation of magnetization is achieved at temperatures 130 and 250 K. The saturation magnetic moment of about 0.17 emu/g was found to be weakly dependent on temperature (see the dashed horizontal lines in Fig. 4). In addition, the magnetization data for the high field range revealed a trace of the diamagnetic behavior (namely, $dM/dH < 0$), which is assumed to be a manifestation of the MWCNT host susceptibility [16]. However, no saturation of $M(H)$ was observed at temperature 5 K. This low temperature branch of $M(H)$ presumably provides an evidence in favor of the paramagnetic behavior of some kind of atomic-scale size Co particles. At high temperatures this paramagnetism appeared to be substantially less pronounced, and one can see that a clear saturation is achieved in the fields above 10 kOe for relatively large ferromagnetic clusters, which are seen in the TEM picture (Fig. 1).

Due to the presence of ferromagnetic clusters, a hysteresis effect in the magnetization was observed in the MWCNT/Co sample, which is presented in Fig. 5 for temperatures 40 and 130 K. The hysteresis loops clearly show that the studied sample is a ferromagnetic material with a comparatively high value of coercive field. The quantitative analysis provides the remanent magnetization value (M_R) of about 0.07 emu/g, which corresponds to 40% of the saturation moment of FM clusters, while the coercive field (H_C) value amounts to 600 Oe. Both quantities M_R and H_C revealed a slight decrease with increasing temperature. Since the value of H_C for a small particle is determined by the product of the particle volume and anisotropy energy, this behavior must be a consequence of high anisotropy energy in the case of Co particles. The observed temperature behavior of the hysteresis effect can be used to estimate roughly the blocking temperature T_B of these
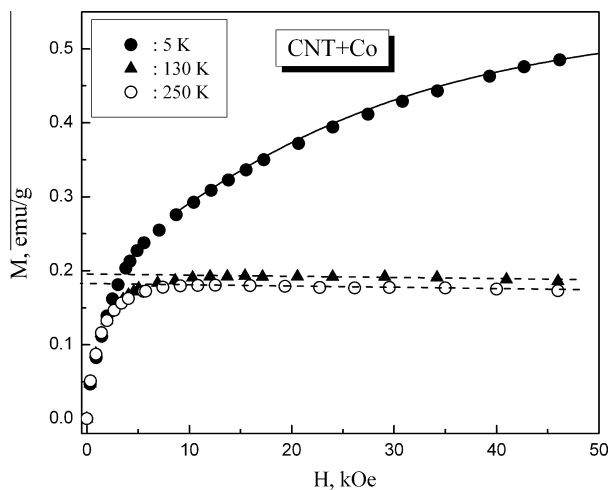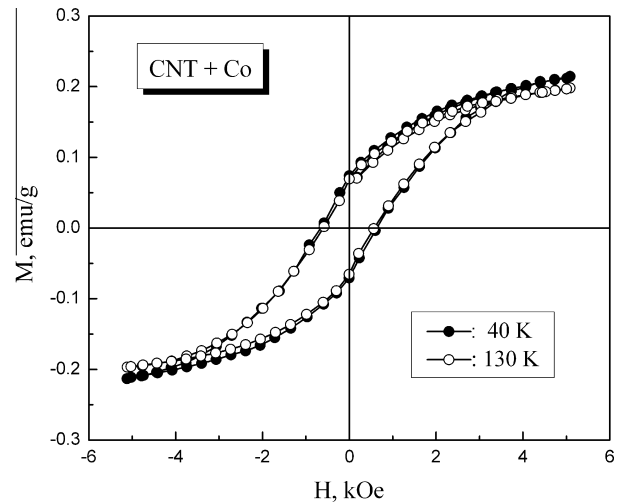

Fig. 5 – Hysteresis effects in magnetization of MWCNT/Co at the temperatures of 40 and 130 K.

magnetic nanoclusters. By using the corresponding formula for the temperature dependence of the coercive field [17]

$$H_C(T) = H_C(0)[1 - (T/T_B)^{1/2}], \qquad (1)$$

we found that the effective blocking temperature for the large Co clusters is well above room temperature. This is also in accordance with the measured in a low field of 300 Oe the temperature dependences of magnetic susceptibility M/H (both ZFC and FC regimes), which are presented in Fig. 6. In fact, the ZFC curve does not show any peak up to 300 K, which could be identified as the blocking temperature. This indicates that produced in this work cobalt nanoclusters with diameter of 10 nm are large enough to exhibit no superparamagnetic behavior below 300 K.

The magnetization increase at low temperatures (clearly seen in Fig. 6) is likely to be due to the very small paramagnetic Co particles, which are presumably much smaller than

Fig. 4 – Magnetization of MWCNT/Co at different temperatures. Model description is presented with the solid line (see text for details).
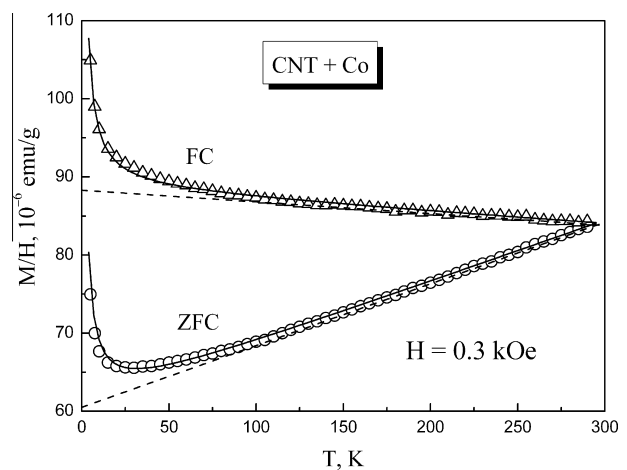

Fig. 6 – The zero field cooled (ZFC) and field cooled (FC) magnetization curves of MWCNT/Co sample versus temperature measured in applied field H of 300 Oe. Model description is presented with the solid lines (see text for details).

those seen in the TEM image (Fig. 1). The magnetic properties of these small particles can be examined, based on the measured magnetization behavior at low temperatures. The magnetization data in Fig. 4 at $T = 5$ K were analyzed for the range of magnetic fields above 10 kOe with the following equation

$$M(H) = n\mu_0 L(x) + M_S, \qquad (2)$$

where $L(x)$ is a Langevin function with $x = \mu_0 H/kT$, n the number of particles, μ_0 their effective magnetic moments, k the Boltzmann constant and M_S the saturated magnetization of FM clusters. Using the experimental data for the saturation magnetic moment at $T = 130$ K (0.19 emu/g, dashed line in Fig. 4) as a rough approximation for the M_S value, a satisfactory description of the magnetization data at $T = 5$ K can be achieved for the fields $H > 10$ kOe with Eq. (2) (see solid line in Fig. 4), by employing the following values of the fitting parameters: $n\mu \cong 0.41$ emu/g and $\mu_0 \cong 5 \times 10^{-2}$ emu. The above values correspond to a concentration of the paramagnetic clusters $n \sim 0.85 \times 10^{19}$ g^{-1} and magnetic moment of one cluster $\mu_0 \sim 5.5\mu_B$ (μ_B is the Bohr magneton).

Furthermore, in Fig. 7 we present the temperature dependence of the magnetization, which was measured in the field $H = 30$ kOe. Based on the above estimations, one can assume, that the low temperature behavior of the $M(T)$ dependence is related to paramagnetism of the magnetic atomic-scale size Co clusters. In order to describe their contribution to the temperature dependence $M(T)$ in Fig. 7, the Langevin function of Eq. (2) was employed again for the temperatures varying in the range of (5–100) K. The solid line in Fig. 7 represents a consistent description of the experimental data on $M(T)$ for $H = 30$ kOe within Eq. (2) with the corresponding fitted parameters: $n\mu_0 \cong 0.39$ emu/g and $\mu_0 \sim 9\mu_B$. These fitted parameters are in a qualitative agreement with those obtained by the analysis of $M(H)$ at $T = 5$ K within Eq. (2) for $H > 10$ kOe (see solid line in Fig. 4). Also, these parameters determine the value of the Curie constant of the paramagnetic clusters, $C = n\mu_0^2/3k \cong 78 \times 10^{-6}$ K emu/g, where n represents their specific number.
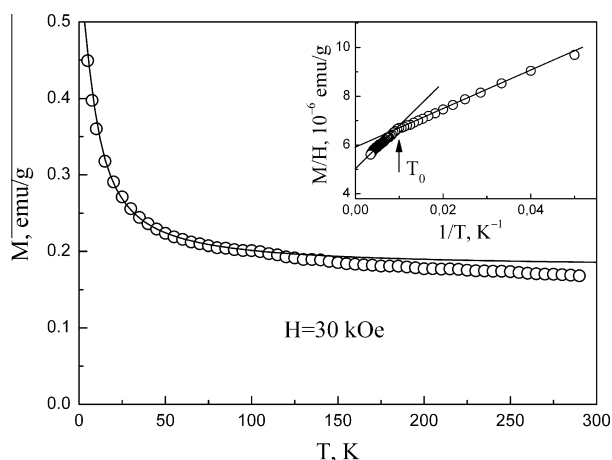

Fig. 7 – Temperature dependence of magnetization for MWCNT/Co measured in field $H = 30$ kOe. Inset: the corresponding M/H dependence as a function of inverse temperature. The Curie–Weiss law approximations are presented with the solid lines (see text for details).

The above obtained value of the paramagnetic Curie constant C can also describe the low temperature behavior of the ZFC and FC magnetic susceptibility measured in $H = 0.3$ kOe (see solid lines in Fig. 6). In this case, however, we assumed the linear temperature dependence of the background magnetization contributions $M_b(T)/H$, which were taken from the experimental data at higher temperatures range (dashed lines in Fig. 6):

$$\chi(T) = C/T + M_b(T)/H. \qquad (3)$$

The magnetization of the MWCNT/Co sample measured in the field $H = 30$ kOe is also presented in the inset in Fig. 7 as a function of the inverse temperature, and it exhibits a crossover at $T \cong 100$ K. The linear dependence for temperatures below 100 K corresponds to the above obtained value of the Curie constant, whereas for the temperatures above 100 K the behavior is close to linear but with the nearly twice higher value of C. The origin of the observed in $M/H(T^{-1})$ inflection point at $T \sim 100$ K (see inset in Fig. 7) is not clear. This can be an indication of the blocking temperature for a small amount of cobalt nanoclusters with an intermediate size, which could produce a superparamagnetic-like behavior above 100 K. Also, one cannot rule out a magnetic phase transition at 100 K for a small amount of residual phase. It should be noted that the peculiarity in magnetization at 100 K was not detected within experimental accuracy in the $(M/H)(T)$ dependence at low field (see Fig. 6) due to the dominance of the ferromagnetic background.

Based on the saturation moment value of about 160 emu/g ($1.6\mu_B$/atom for bulk metallic cobalt), we can roughly estimate the amount of Co in "large" FM clusters to be ~ 0.12 wt.%, using the value of their saturation moment of about 0.19 emu/g. To evaluate in a similar way a fraction of paramagnetic nanoparticles in the sample, we need to know the number of constituent atoms of cobalt. Comparing the obtained value $\mu_0 \sim (5.5–9)\mu_B$ with the theoretical estimations of magnetic moments of Co in atomic-scale size particles ($\sim 2\mu_B$/atom, [18]), we can roughly estimate that the paramagnetic nanoparticle consists of (3–5) Co atoms. Accordingly their total amount is about (0.3–0.5)% of the sample mass. Therefore, for the sample under study the overall cobalt content in the FM clusters and atomic-scale size paramagnetic particles amounts to about (0.4–0.6) wt.%.

4. Conclusions

Synthesized MWCNTs modified with cobalt (MWCNT/Co) were investigated with respect to their structural and magnetic properties. SEM and HRTEM studies show that MWCNTs have the inner diameter about 10–12 nm, whereas the outer diameter is about (30–40) nm and the length is up to 40 μm and contains clusters of cobalt (or its compounds) with average diameter 5 nm. The SEM and HRTEM results demonstrate the absence of amorphous carbon and graphitic particles in the samples. The XRD study revealed the f.c.c. and h.c.p. cobalt phases, as well as the carbon phase, present in the MWCNT/Co sample, whereas characteristic reflections of related oxides or carbides were not detected.

Magnetization studies revealed two principal groups of Co nanoclusters in the synthesized MWCNT/Co sample. The larger particles have a size from a few to about 10 nm. They are ferromagnetic, at least up to 300 K, with the coercive field of about 600 Oe. The smaller Co particles have the atomic-scale size. They are responsible for a pronounced paramagnetic behavior observed at low temperatures.

REFERENCES

[1] Dresselhaus MS, Dresselhaus G, Eklund PC. Science of fullerenes and carbon nanotubes. New York: Academic Press; 1996.

[2] Harris PJF. Carbon nanotubes and related structures. Cambridge: Univ. Press; 1999.

[3] O'Connell M, editor. Carbon nanotubes: properties and applications. NY: Taylor and Francis Group; 2006.

[4] McIntosh GC, Kim GT, Park JG, Krstic V, Burghard M, Jhang SH, et al. Orientation dependence of magneto-resistance behavior in a carbon nanotube rope. Thin Solid Films 2002;417(1–2):67–71.

[5] Cottet A, Kontos T, Sahoo S, Man HT, Choi MS, Belzig W, et al. Nanospintronics with carbon nanotubes. Semicond Sci Technol 2006;21(11):78–95.

[6] Tyagi PK, Singh MK, Misra DS, Ghatak J, Satyam PV, Le Normand F. High-resolution transmission electron microscopy mapping of nickel and cobalt single-crystal nanorods inside multi-walled carbon nanotubes and chirality calculations. Appl Phys Lett 2005;86(25):253110–2.

[7] Borowiak-Palen E, Ruemmeli MH, Gemming T, Pichler T, Kalenczuk RJ, Silva SRP. Silver filled single-wall carbon nanotubes: synthesis, structural and electronic properties. Nanotechnology 2006;17(9):2415–9.

[8] Ovsienko I, Len T, Matzui L, Prylutskyy Yu, Eklund P, Le Normand F, et al. Transport properties of carbon nanotube–metal nanocomposites. Physica E 2007;37(1–2):78–80.

[9] Mykhailenko OV, Hui D, Strzhemechny YuM, Matsui D, Prylutskyy Yui, Eklund P. Monte Carlo simulations for carbon nanotubes intercalated with different atomic species. J Comput Theor Nanosci 2007;4(6):1–4.

[10] Ovsienko IV, Matzuy LYu, Zakharenko MI, Babich MG, Len TA, Prylutskyy YuI, et al. Magnetometric studies of nanocarbon materials containing carbon nanotubes. Nanoscale Res Lett 2008;3(2):60–4.

[11] Grechnev GE, Desnenko VA, Fedorchenko AV, Panfilov AS, Matzui LYu, Prylutskyy YuI, et al. Structure and magnetic properties of multi-walled carbon nanotubes modified with iron. Low Temp Phys 2010;36(12):1347–51.

[12] Grobert N, Hsu WK, Zhu YQ, Hare JP, Kroto HW, Walton DRM, et al. Enhanced magnetic coercivities in Fe nanowires. Appl Phys Lett 1999;75(21):3363–5.

[13] Wang ZH, Choi CJ, Kim BK, Kim JC, Zhang ZD. Characterization and magnetic properties of carbon-coated cobalt nanocapsules synthesized by the chemical vapor condensation process. Carbon 2003;41(9):1751–8.

[14] El-Gendy AA, Ibrahim EMM, Khavrus VO, Krupskaya Y, Hampel S, Leonhardt A, et al. The synthesis of carbon coated Fe, Co and Ni nanoparticles and an examination of their magnetic properties. Carbon 2009;47(6):2821–8.

[15] Lyakhno VY, Fedorchenko AV, Kivirenko OB, Shnyrkov VI. FRP Dewar for measurements in high pulsed magnetic fields. Cryogenics 2009;49(8):425–8.

[16] Lipert K, Kretzschmar F, Ritschel M, Leonhardt A, Klingeler R, Büchner B. Nonmagnetic carbon nanotubes. J Appl Phys 2009;105:063906-1–063906–4.

[17] Kneller EF, Luborsky FE. Particle size dependence of coercivity and remanence of single-domain particles. J Appl Phys 1963;34(3):656–8.

[18] Bennemann K. Magnetic nanostructures. J Phys: Condens Matter 2010;22(24):243201-1–243201–39.